Symmetry Plane Viscous Layer on a Sharp Cone

S. G. Rubin,* T. C. Lin,† and F. Tarulli‡
Polytechnic Institute of New York, Farmingdale, N. Y.

Numerical solutions for the wind and lee symmetry planes on sharp cones at incidence are obtained for laminar boundary layers. Comparisons are made between solutions obtained with the similarity boundary-layer equations, the nonsimilar boundary-layer equations, and the nonsimilar boundary region equations. For moderate incidence angles, boundary-layer theory fails at the leeplane and a boundary region develops. For large incidence, after crossflow reversal has occurred, nonsimilar boundary-layer solutions are obtained at the leeplane but are in poor agreement with experimental data. The boundary region system provides a significant improvement.

I. Introduction

THE cone at angle of attack has served as a prototype for many investigations of three-dimensional boundary layers in supersonic flows. These studies can be categorized as: 1) similar boundary layer,[1-11] 2) nonsimilar boundary layer,[12-15] and 3) nonsimilar boundary region[16-18] § analyses.

With approximations 1 and 2, it has been shown[1] that the symmetry plane equations uncouple from the interior system so that for weak viscous-inviscid interaction the wind- and leeplane flow histories are apparently independent of the boundary-layer behavior around the cone. Solutions for the leeplane boundary layer therefore can be obtained by direct integration of the uncoupled symmetry plane equations[1-6] (ordinary differential equations), or, alternatively, by a wind-to-leeplane marching procedure[7-15] using the partial differential system governing the three-dimensional similarity boundary layer. The windward boundary-layer solution, as obtained from the uncoupled system, serves as the initial condition for the marching integration. For group 3 problems this uncoupling is not possible as diffusion effects are important not only normal to the surface, as with boundary layers, but also normal to the symmetry or separation planes. These domains, where a boundary layer forms within a boundary layer, are nonsimilar and termed boundary regions. Solutions of the nonsimilar boundary region equations can be obtained only by a streamwise integration procedure. Boundary-layer profiles are not specified at either of the symmetry planes.

For unseparated flows, i.e., small to moderate angles of incidence, the boundary-layer methods of categories 1 and 2 have failed to provide leeplane solutions for all but the smallest yaw angles. This difficulty is most apparent with the uncoupled symmetry plane studies, as the calculations have failed to converge,[1-6] but even with the complete boundary-layer integration starting at the windplane, anomalous leeplane behavior has been observed.[7-13] Moreover, the similarity symmetry plane equations exhibit nonunique windward plane solutions for all incidence angles. This nonuniqueness prevails at the leeplane in the limited range where solutions have been obtained.

For separated flows,¶ i.e., larger incidence angles, boundary-layer wind-to-leeplane marching procedures encounter the familiar difficulties associated with numerical integration into reverse flow regions. Surprisingly, uncoupled solutions for both the similar and nonsimilar boundary layers at the symmetry planes reappear at the larger yaw angles. The similarity results are not unique, however, and in addition, for both similar and nonsimilar systems, the accuracy of even the best of these results does not appear to be acceptable. Moreover, at certain very large incidence angles anomalous behavior is observed in the flow profiles of the similarity boundary-layer solutions.

Boundary region solutions, for both separated and attached flows, have been obtained and are in good agreement with the available experimental data. In the present paper, the symmetry plane behavior will be analyzed and reasons for the success or failure of the approximations previously delineated will be discussed.

II. Governing Equations

The governing equations for three-dimensional boundary-layer and boundary region flows have been derived and discussed in previous studies[12-18] and, therefore, only a brief description is presented here.

A. Boundary Region

The most general form of the boundary region equations is presented in Refs. 17 and 23. For high Reynolds number flow, neglecting centrifugal pressure effects, it is assumed that $\partial/\partial y >> \partial/\partial x$ so that: 1) $p_y = 0$, and 2) streamwise diffusion terms can be neglected (see Fig. 1).

The equations are nonsimilar and allow for boundary region formation so that crossflow diffusion terms are retained. With diffusion normal to the symmetry planes retained in the governing system, the symmetry plane flow cannot be uncoupled from the interior flow calculation. Therefore, wind- and leeplane solutions have been obtained from complete flowfield calculations.[17]

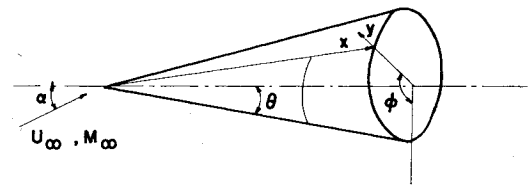

Fig. 1 Cone geometry.

Received July 13, 1976; presented as Paper 76-362 at the AIAA 9th Fluid and Plasma Dynamics Conference, San Diego, Calif., July 14-16, 1976; revision received Nov. 12, 1976.

Index categories: Boundary Layers and Convective Heat Transfer—Laminar; Supersonic and Hypersonic Flow.

*Professor of Aerospace Engineering, Aerodynamics Laboratories. Associate Fellow AIAA.

†Currently at Avco Missile Systems Division, Wilmington, Mass. Member AIAA.

‡Currently at Sikorsky Aircraft Corp., Div. of United Technologies, Stratford, Conn.

§Shock layer methods, where the inviscid and boundary-layer flows are calculated as a single layer, are included here as well.

¶Flow reversal and vortex formation in the plane normal to the cone axis.

B. Boundary Layer

If the cross-diffusion effects retained in Sec. II A are neglected, we recover the familiar three-dimensional boundary-layer equations.[12] Solutions of these equations are obtained by either streamwise integration, incorporating a wind-to-leeplane marching procedure[12-15] at each streamwise location, or by direct integration of the now uncoupled symmetry plane equations given for unit Prandtl number as follows

$$f_{\eta\eta\eta} + (f+Kg)f_{\eta\eta} = 2\xi(f_\eta f_{\eta\xi} - f_\xi f_{\eta\eta}) \tag{1a}$$

$$g_{\eta\eta\eta} + (f+Kg)g_{\eta\eta} + K[(\rho/\rho_e) - f_\eta g_\eta] = 2\xi(f_\eta g_{\eta\xi} - f_\xi g_{\eta\eta}) \tag{1b}$$

$$\Theta = f_\eta \tag{1c}$$

$$\rho_e/\rho = (1+m)[H_w + (1-H_w)f_\eta] - mf_\eta^2 \tag{1d}$$

where

$$m = (\gamma-1)M_e^2/2,\ h = H/H_e$$

$$K = 2/3\frac{w_{e\varphi}}{u_e \sin\theta},\ \frac{\rho\mu}{(\rho\mu)_e} = 1$$

$$u/u_e = f_\eta,\ w_\varphi/w_{e\varphi} = g_\eta$$

$$\Theta = (H-H_w)/(H_e-H_w)$$

$$\eta = \left(\frac{3\rho_e\mu_e}{2x\mu_e}\right)^{1/2}\int_o^y \frac{\rho}{\rho_e}dy$$

$$\xi = \rho_e\mu_e u_e x^3 \sin^2\theta/3$$

$$\theta = \text{cone half angle}$$

H is the stagnation enthalpy defined as $c_pT + [(u^2+w)^2/2]$. The coordinates and geometry are depicted on Fig. 1. e denotes boundary layer edge values. w denotes wall values. The boundary conditions are

$$\eta = 0: \quad f = f_\eta = g = g_\eta = 0$$

$$\eta \to \infty: \quad f_\eta,\ g_\eta,\ \Theta \to 1 \tag{1e}$$

Solutions of the system (1) will be discussed later in this report.

C. Similar Boundary Layer

Finally, the system described in Sec. II B can be simplified further by requiring that the similarity condition $\partial/\partial\xi = 0$ be imposed. Streamwise marching is no longer necessary and solutions can be obtained either by wind-to-leeplane integration or by direct solution of the ordinary differential equations of the uncoupled symmetry plane flow;[1-6] i.e., Eqs. (1) with $\partial/\partial\xi = 0$. With $\partial/\partial\xi = 0$, the similarity system (1) exhibits the following asymptotic behavior[1] for $\eta >> 1$ and K = constant

$$f''(\eta) \sim \exp -(1+K)\eta^2/2 \tag{2a}$$

$$g'(\eta) \sim [\exp -(1+K)\eta^2/2][\eta(1+K)^{1/2}]^{-3(K+5/9)/(1+K)} + \sigma((1+K)^{1/2}\eta)^{2(K+1/3)/(1+K)} \tag{2b}$$

where σ is a constant. Asymptotic expressions for (1a) with $\partial/\partial\xi \neq 0$ are derived in Sec. III C.

III. Analysis

A. Similarity-Symmetry Plane Equations

The symmetry plane boundary layer as governed by system (1) has been considered in a number of investigations. Moore[1] was the first to examine these equations in detail, and from the asymptotic formulas (2) he inferred the following. At the inflow or leeplane ($K<0$), 1) for very large incidence $K<-1$, a solution of the system (1) should not be possible as the asymptotic flow grows exponentially. This is indicative of a breakdown of either the similarity approximation or of boundary-layer theory. 2) For $-1/3 > K > -1$, the asymptotic decay is partially algebraic. This leads to an eigenvalue problem for the algebraic behavior and therefore Moore concluded that the solutions would not be unique in this range of K. Furthermore, for $K<-2/3$, the appearance of an adverse pressure gradient in the aximuthal (φ) direction was indicative of crossflow reversal and vortex formation for these incidence angles. 3) For $K \geq -1/3$, the solutions all exhibit exponential decay; however, with arguments based on the domain of dependence of the symmetry plane flow, Moore inferred a possible nonuniqueness for all but the smallest incidence angles; i.e., $K > 1/3 f''(0)/g''(0)$. At the windward (or outflow) plane ($K>0$), Moore predicts unique solutions with exponential decay for $K>0$.

Subsequently, Cheng,[2] Roux,[3] Murdock,[4] and Wu and Libby,[5] with numerical investigations of the system (1), reported the existence of two distinct single-branch solutions for $K \geq -K^*$, including all $K \geq 0$. The value of K^* is dependent upon the wall temperature ratio $g_w = H_w/H_e$ and the Mach number parameter, $m = [(\gamma-1)/2]M_e^2$ or $\bar{m} = m/(1+m)$. Murdock considered only the case $m = 8.0$ or $\bar{m} = 0.889$, $g_w = 0.4$. For these values, $K^* = 0.079$. Wu and Libby present extensive calculations for values of $\bar{m} = 0$, 0.714, 1, and $g_w = 0$, 1, 2. For $\bar{m} = 0$, $g_w = 1$, $K^* \sim 0.3$; for $\bar{m} = 0.714$, $g_w = 0.1$, $K^* \approx 0.27, 0.13$.

Of the two branch solutions found for $K > -K^*$, the upper branch value coincides with the well-known solutions of Moore[1] and Reshotko.[6] These solutions are regular as $K \to 0$. The lower branch solutions are singular for $g_w > 0$ and $0 < K << 1$. Roux[3] discounts these solutions as physically unacceptable, but Wu and Libby believe that these profiles can be established with appropriate suction boundary conditions. For the present analysis only nonporous walls are considered and therefore we would expect to find the upper branch solutions for $K > -K^*$.

For angles of incidence $-\tilde{K} < K < -K^*$, solutions for the leeplane boundary cannot be obtained with the similarity symmetry plane equations. As noted by Wu and Libby, the value of $\tilde{K}$ is approximately 2/3. For the conditions considered by Murdock, $\tilde{K} = 0.6656$.

For large angles of incidence $-1 < K < -\tilde{K}$, Murdock and Wu and Libby were able to solve the leeplane symmetry equations once again; however, a double-valued solution was found by Murdock and two double-valued branches were obtained by Wu and Libby. It is quite possible that additional eigensolutions occur. The reader is referred to these papers and to the article by Roux[3] for further discussion of the wind- and leeplane multi-valued solutions.

Because of the asymptotic exponential growth exhibited in (2), values of $K<-1$ have not been considered previously. These cases have been considered here and the following interesting results have been obtained. As shown on Figs. 2-4, similarity boundary-layer profiles have been generated for $K<-1$. These results represent solutions of Eqs. (1) with $\partial/\partial\xi = 0$ and with the outer boundary conditions $|f'-1| < 10^{-3}$ and $|g'-1| < 10^{-3}$. These asymptotic values, for $K = 1.35$, are achieved at $\eta = 3.5$ for f' and $\eta = 12.5$ for g'. The streamwise velocity (f') boundary layer is considerably thinner than that found for the crossflow (g'). This behavior is apparent in all of the solutions for $K<-1$. The asymptotic solutions for f appear to exhibit exponential decay in contradiction with the asymptotic growth predicted by Moore [see Eqs. (2)]; e.g., from Table 1 at $\eta = 20$, $f'' = 0(10^{-24})$.

In order to assess the behavior for $\eta >> 1$, the problem was reconsidered as an initial value problem with the values of

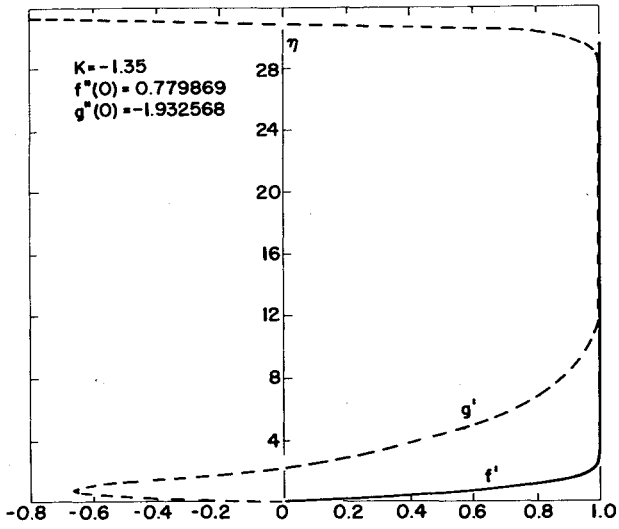

Fig. 2 Similar boundary layer: velocity profiles at leeplane.

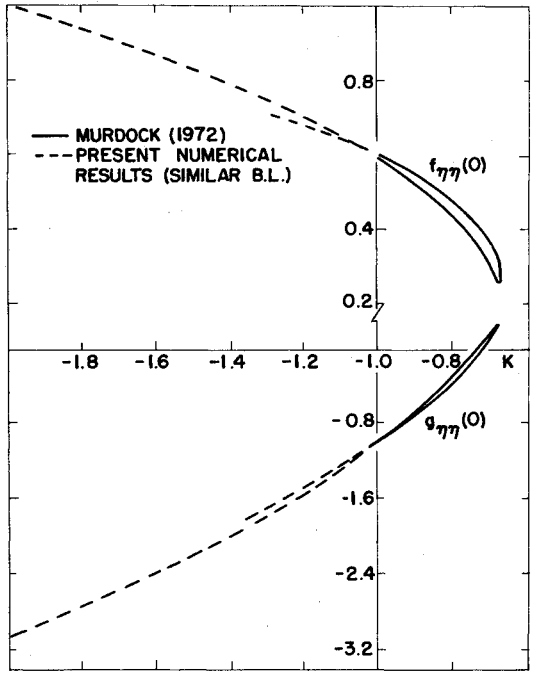

Fig. 3 Similarity solutions at leeplane for large incidence angles.

Table 1 Similar solution: $K=-1.35$

η	f	f'	g	g'
0	0	0	0	0
1	0.3732	0.7030	-0.5242	-0.6467
2	1.2464	0.9698	-0.9113	-0.1253
4	3.2360	0.9997	-0.5344	-0.4269
6	5.2354	0.9997	0.6502	0.7301
8	7.2348	0.9997	2.2917	0.8924
12	11.2335	0.9997	6.1252	0.9932
16	15.2323	0.9997	10.1223	1.0011
20	19.2310	0.9997	14.1264	1.0011
24	23.2298	0.9997	18.1303	1.0010
28	27.2286	0.9997	22.1329	0.9975
29	28.2283	0.9997	23.1254	0.9843
30	29.2283	0.9997	24.0821	0.9028
31	30.2277	0.9997	24.7030	-0.0401
32	31.2274	0.9997	19.7229	-17.7787
33	32.2270	0.9997	-104.2813	-401.9318

f"(0) =0.77987
g"(0) =-1.93257

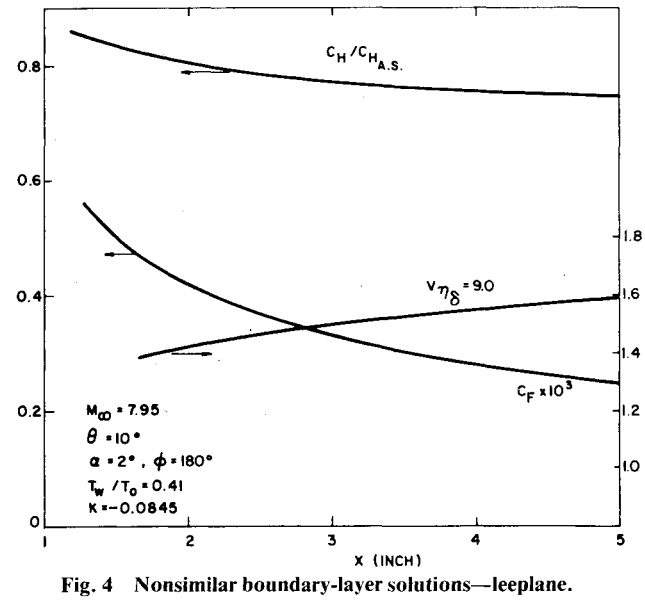

Fig. 4 Nonsimilar boundary-layer solutions—leeplane.

$f''(0)$ and $g''(0)$ obtained from the solution previously discussed. The complete profiles shown on Fig. 2 and Table 1 for $K=-1.35$ demonstrate that for $\eta>>1$, the g profile does increase exponentially after passing through a significant region where $g\sim\eta-\beta_2$; e.g., for $K=-1.35$, this region extends from $\eta=12.5$ to $\eta=24$. Similar behavior is observed for all other values of $K<-1$ that were considered. Surprisingly, the f profiles maintain a strong exponential decay with $f\sim\eta-\beta_1$ throughout. The reason for this behavior can be seen in the solutions for $f+Kg$. Exponential decay in (2) is predicted when $f+Kg>0$. For $\eta>>1$, $f+Kg\sim\eta(1+K)-\beta_1-K\beta_2$, and with $K<-1$, $f+Kg<0$ for some $\eta>>1$. However, over a significant range of $\eta>1$, $f+Kg>0$ and exponential decay is maintained. For $K=-1.35$, $\beta_1=5.87$ and $\beta_2=0.77$. Therefore, $f+Kg>0$ when $(1+K)\eta-0.77+(1.35)(5.87)<0$ or $\eta>20.44$. Only for $\eta<20.44$ is exponential growth observed. The solutions for $\eta<20.44$ appear to be reasonable similarity boundary-layer profiles with asymptotic exponential decay.

For $\eta>>1$, the asymptotic equation (2) becomes $gg''=g'^2$ so that $g\sim Ae^{B\eta}$, A, $B>0$. With $g<0$, $f+Kg$ is once again positive so that f exhibits exponential decay even as g grows. This behavior is evident from the results on Table 1. Therefore the streamwise profile is acceptable for all η, whereas a singular behavior in g' is observed only for $\eta>>1$ ($\eta>24$ for $K=-1.35$). Similar results have been obtained for other values of $K<-1$.[22] In addition, a second branch also has been detected for $K<-1$. The profiles (not shown) closely resemble those of the first branch. As shown on Fig. 3, the two distinct solutions represent continuations for $K<-1$ of the double-valued results found by Murdock for $K>-1$. Extensions of the second branch found by Wu and Libby were not considered specifically and the existence of other eigensolutions for $K<-1$ cannot be dismissed.

The solutions for $K<-1$ appear to be well behaved for moderate η values with the similarity approximation applying over a major portion of the boundary layer. The singular behavior encountered for $\eta>>1$ signals a failure of the similarity equations. This will be seen more clearly in Sec. III B where the nonsimilar system is considered.

In summary, the uncoupled similarity equations governing the boundary layer in the symmetry planes provide solutions at the windward plane for all incidence angles, and at the leeplane only in certain ranges of the parameter K, e.g., $K>-K^*$ and $-1<K<-\bar{K}$. For $K<-1$, novel boundary-layer solutions ultimately growing exponentially have been found. Moreover, when solutions have been obtained, they are not unique. This is true at both the wind- and leeplanes.

B. Similarity Wind-to-Leeplane Boundary Layer Integration

Solutions of the symmetry plane equations (1) are found at the windward plane ($K>0$) in order to initiate a marching procedure for the complete similarity system[8-11] around to the leeplane. Although the windplane solutions are double-valued, only one branch is physically acceptable without some form of slot injection or suction on the cone surface (see Roux,[3] Wu and Libby[5]). It is this solution, which agrees well with available experimental data, that is used as the initial profile. Marching solutions for the similarity equations have been obtained by Cooke,[8] Boericke,[9] Roux,[10] and Tarulli.[11] For small angles of incidence, solutions for the leeplane boundary exist and are in agreement with continuous branch solutions of the symmetry plane equations for $K>-K^*$ (see Wu and Libby[5]). As the incidence angle increases, but prior to crossflow reversal, solutions at the leeplane no longer can be obtained. One possible reason for this failure is noted in many of the previous investigations. The velocity component around the cone does not vanish as the leeplane is approached. It would appear that the mass entering the leesurface cannot be accommodated by a boundary-layer growth compatible with the similarity approximation, i.e., $\delta \sim x^{1/2}$. The results to be presented later in this paper (Sec. III D) will demonstrate this postulate clearly.

Once crossflow reversal and vortex formation occurs, the marching procedures terminate prior to the leesurface and therefore cannot provide any further information about the leeplane boundary layer.

C. Nonsimilar Boundary-Layer Marching

If the similarity approximation is relaxed, the system (1) is recovered. Once again the equations along the symmetry planes uncouple from the interior flow and, in principle, can be solved independently. Solutions of this system are discussed later in this section. As with the similarity equations, solutions of the entire system[12,13] also can be obtained by wind-to-leeplane integration. The initial profiles at the windward plane are determined, for all incidence angles, from the nonsimilar symmetry plane equations (1).

Since the governing system is nonsimilar the equations also must be integrated in the streamwise direction (along the x-axis or cone ray). The initial integration is made along the independent windward plane and then sequentially around the cone until the leeplane or crossflow reversal is encountered. Calculations of this type for laminar flow have been described by McGowan and Davis[12] and Dwyer.[13] The details of their integration procedures will not be described as we are only concerned here with the symmetry plane behavior. In this regard, the results can be summarized as follows.

For the symmetry equations (1) solutions at the windward surface can be found for all incidence angles. Typical solutions are shown in Fig. 4. *A.S.* denotes axisymmetric conditions ($\alpha=0°$) and η_δ is the η value at the boundary-layer edge. For similar flows, η_δ is constant. These nonsimilarity solutions are unique and appear to correspond to the lower values on the continuous branch found by Roux, Murdock, and Wu and Libby with the similarity equations discussed in Sec. III A.

Unique solutions at the leeplane, all exhibiting exponential decay for $\eta>>1$, are found for small angles of attack as well as for large incidence angles, Figs. 4-6. Once again a region roughly corresponding to $-\tilde{K}<K<-K^*$ exists for which a physically acceptable solution is not found. The flow behavior in this range of K is indicated on Fig. 7. Note that as ξ increases, the boundary layer continually thickens and the heat transfer and skin friction decrease until "separation" occurs. This is not observed experimentally and therefore it must be concluded that for $-K<K<-K^*$ it is not the similarity approximation that fails, but that weak interaction boundary-layer theory itself is no longer valid. In Sec. III D, the weak interaction boundary region analysis is presented. Conical flow solutions are obtained for all K values, confirming the inadequacy of ordinary boundary-layer approximations for a range of incidence angles. Figure 6 also depicts these boundary region calculations. The heat transfer exhibits a similarity behavior, but the boundary-layer thickness η_δ is nonsimilar.

Significantly, nonsimilar conical flow solutions are found even for very large incidence, i.e., $K<-1$, indicating that the failure of the similarity equations for large yaw angles is associated not with a failure of boundary-layer theory but with the failure of the similarity approximation. Solutions are shown on Figs. 5 and 6. The inner boundary layer and surface properties are virtually invariant with ξ; i.e., similarity holds over most of the boundary layer. Only in the outer portions of

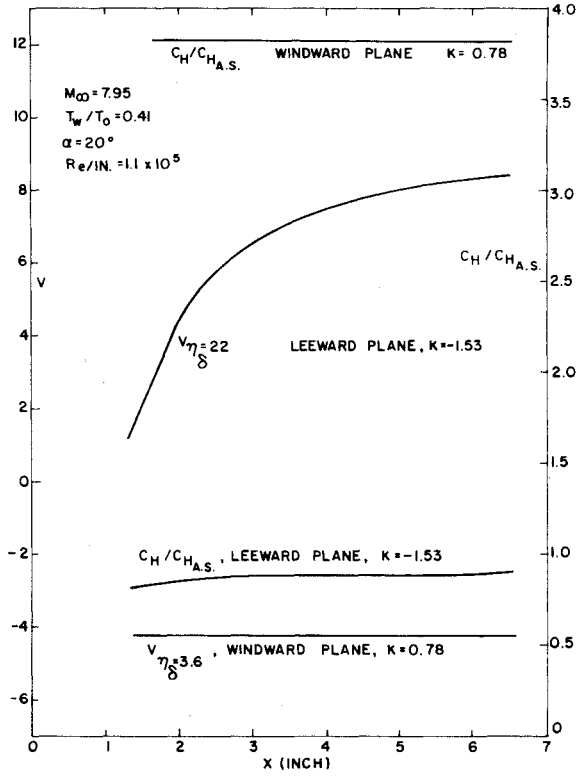

Fig. 5 Nonsimilar boundary-layer solutions.

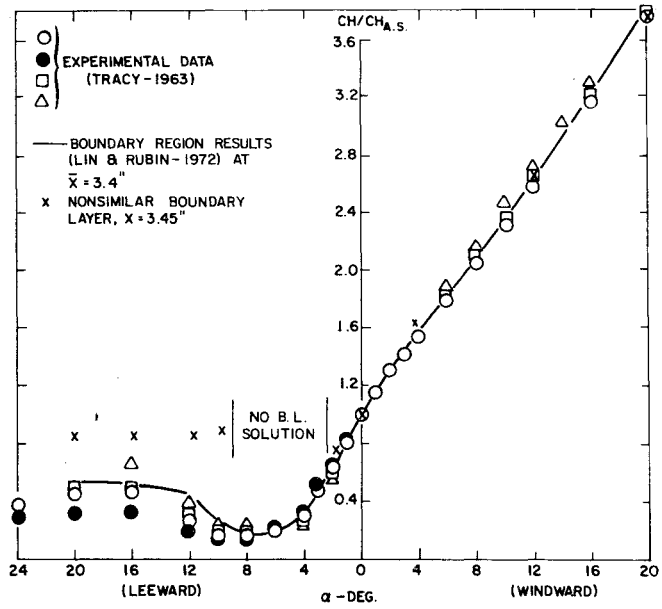

Fig. 6 Heat transfer at symmetry plane.

the boundary layer is a slight nonsimilar growth detected. This behavior concurs with the similarity solutions of Sec. III A. As shown on Fig. 6, the heat-transfer results do not, however, agree well with the data. As seen in Sec. III D, boundary region corrections are also important for large $-K$.

The anomalous behavior for $K<-1$ found in Sec. III A can be explored with the following approximate analysis of the nonsimilar equations. Consider the nonsimilar symmetry plane equations (1). If $f(\xi,\eta)=f(\eta)$, $g(\xi,\eta)=g(\eta)$, the boundary conditions (1e) predict that for $K<-1$ the asymptotic solution (2) grows exponentially. As we have seen, similar solutions of the boundary-layer equations with exponential decay have been obtained. The streamwise velocity profiles are well defined and the cross velocity deteriorates only for very large values of η. Since the nonsimilar, conical solutions are well defined and closely approximate the similarity solutions for small and moderate values of η, it appears that the similarity form fails only in the outer regions of the boundary layer.

The effects of the nonsimilar terms in Eqs. (1a) and (1b) can be evaluated with the following asymptotic analysis. Assume

$$f(\xi,\eta)\sim\eta-\beta_1+F(\xi,\eta)$$

$$g(\xi,\eta)\sim\eta-\beta_2+G(\xi,\eta)$$

where F,G are exponentially small terms for η, $\xi>>1$. The similarity solutions are recovered if, for $\xi\to\infty$, $F(\xi,\eta)\sim F(\eta)$ and $G(\xi,\eta)\sim G(\eta)$. Equation (1a) for η, $\xi>>1$ can be written as

$$F_{\eta\eta\eta}+[(K+1)\eta-(\beta_1+K\beta_2)]F_{\eta\eta}=2\xi F_{\eta\xi} \tag{3}$$

Differentiating with respect to η, we obtain the following equation for $S=F_{\eta\eta}$

$$S_{\eta\eta}+[(K+1)\eta-(\beta_1+K\beta_2)]S_\eta+(K+1)S=2\xi S_\xi \tag{4}$$

A solution of (4) takes the form

$$S=A(\xi)\exp\{-(K+1)[1+C(\xi)]\eta^2/2 + (\beta_1+K\beta_2)[1+D(\xi)]\eta\} \tag{5}$$

where

$$-\xi C'(\xi) = (K+1)[C+C^2] \tag{6a}$$

$$2\xi A'/A = -(K+1)C+(D^2+D)(\beta_1+K\beta_2)^2 \tag{6b}$$

$$2\xi D'/A = -(K+1)[C+(1+2C)D] \tag{6c}$$

1) For $K>-1$, $C=\alpha\xi^{-(K+1)}/[1-\alpha\xi^{-(K+1)}]$ so that $C\to 0$ as $\xi\to\infty$. In this case the dominant term is exponentially decaying; $A\sim\sigma_1=$constant, and $D\sim\sigma_2\xi^{-(K+1)/2}\to 0$ as $\xi\to\infty$. Therefore, Eq. (5) becomes

$$S\sim\sigma_1\exp[-(K+1)\eta^2/2+(\beta_1+K\beta_2)\eta]$$

σ_1, σ_2 are constants. The similarity form (2a) is recovered as it should be in this range of K.

2) For $K=-1$, $C=\alpha_1=$constant. With $D=0$ and $A=\alpha_2=$ constant, we have $S\sim\alpha_2\exp(\beta_1-\beta_2)\eta$. The numerical solutions for $K=-1$ clearly demonstrate that $\beta_1-\beta_2<0$. In fact, $\beta_1=0.92$, $\beta_2=3.03$, so that, once again, similarity form is applicable.

3) For $K<-1$, $C=\alpha_3(\xi^{(K+1)}-\alpha_3)^{-1}$ where $\alpha_3>0$. As $\xi\to\infty$, $C\to-1$, and $1+C\sim-\xi^{K+1}/\alpha_3$. Asymptotic solutions for $A(\xi)$ and $D(\xi)$ as obtained from Eq. (6) are

$$A(\xi)\sim\alpha_4\xi^{(K+1)/2}+0(\xi^{K+1})$$

$$D(\xi)\sim\alpha_4\xi^{(K+1)/2}+0(\xi^{K+1})$$

Therefore, A, $D\to 0$, as $\xi\to\infty$ for $K<-1$. The nonsimilar asymptotic solution (5) for S becomes, for η, $\xi>>1$,

$$S\sim\xi^{(K+1)/2}\{\exp[(K+1)\eta^2\xi^{K+1}/2\alpha_3]+(\beta_1+K\beta_2)\eta\}$$

For $\xi\to\infty$ and $\beta_1+K\beta_2<0$, all terms exhibit exponential decay. As can be inferred from the solution on Table 1, $\beta_1+K\beta_2<0$. The exponential growth (2a) found with the similarity equations is suppressed by the nonsimilar terms in (1) so that the resulting solution exhibits exponential decay. These nonsimilar terms are very small for η, $\xi>>1$ but play a critical role in the asymptotic field. The numerical solutions for the nonsimilar system are in good agreement with this approximate analysis. In the interior regions the flow appears to be similar. Only in the outer boundary layer for large η do small streamwise gradients persist in the ξ integration. This may explain, in part, the unusual results obtained for $K<-1$, with the similar boundary-layer equations of Sec. III A.

The failure of even the nonsimilarity boundary-layer approximation for moderate incidence, approximating the range $-\tilde{K}<K<-K^*$, and prior to crossflow reversal and vortex formation, is confirmed also with the wind-to-leeplane marching calculations. Acceptable solutions have not been obtained for these yaw angles. See Popinski and Davis[12] for a discussion of the anomalous leeplane behavior. For larger incidence, crossflow reversal occurs and the leeplane is not calculated by the nonsimilarity marching procedures.

D. Boundary Region Analysis

The equations governing the symmetry plane boundary region are given in Refs. 16 and 17. The boundary region theory assumes that a thin high-gradient region forms about the symmetry plane. In this region diffusion is important not only normal to the surface (y direction), but also normal to the symmetry plane (φ direction). Boundary regions previously have been discussed for corner regions[19] and for edge or tip regions.[20] The boundary region, which constitutes a boundary layer within a boundary layer, is generally created by a crossflow boundary condition that cannot be satisfied in the usual context of ordinary boundary-layer theory. These boundary values are rather evident for the corner with perpendicular interference walls and for the edge where a discontinuity of boundary value occurs. For the cone symmetry plane the formation of a boundary region is not obvious, although the inflow or leeplane symmetry line is in

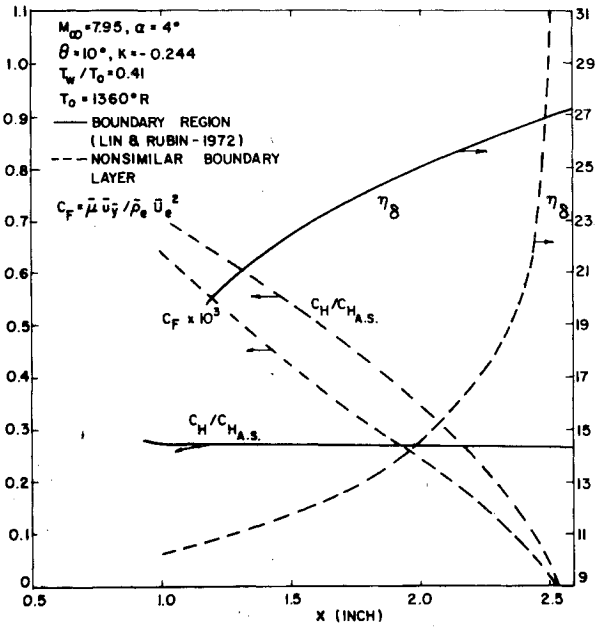

Fig. 7 Nonsimilar boundary-layer and boundary-region solutions.

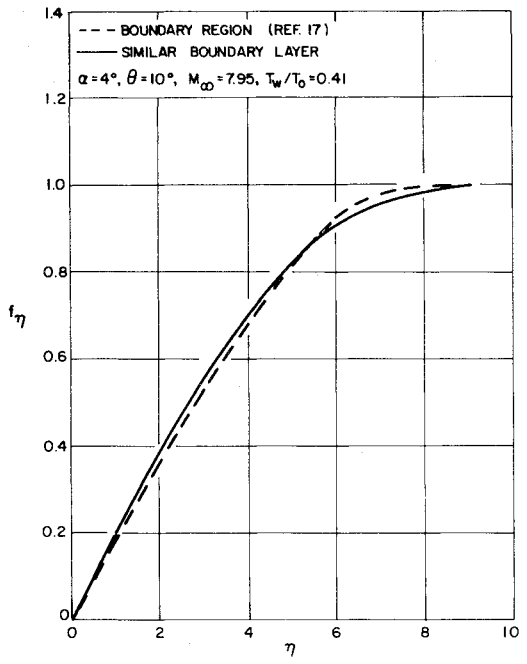

Fig. 8 Streamwise velocity distribution, $\phi = 170°$.

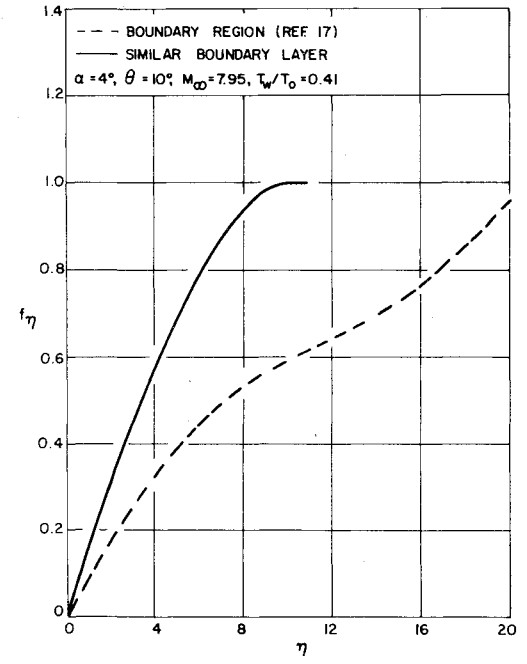

Fig. 9 Streamwise velocity distribution, $\phi = 179°$.

Table 2 Crossflow—similar boundary-layer marching

ϕ (DEG.)	$(g_\eta)_{MAX}$	w_{MAX} (FT./SEC.)
0.0	1.5887	0.0
10.0	1.6095	40.0
20.0	1.6150	80.0
30.0	1.6242	120.0
40.0	1.6375	159.0
50.0	1.6551	197.0
60.0	1.6775	232.5
70.0	1.7052	266.0
80.0	1.7389	296.0
90.0	1.7791	320.5
100.0	1.8278	338.0
110.0	1.8865	347.5
120.0	1.9588	344.0
130.0	2.0512	332.0
140.0	2.1767	304.0
150.0	2.4175	269.0
160.0	2.8445	221.0
170.0	3.8754	154.0
172.0	4.3240	138.5
174.0	5.0213	121.0
176.0	6.3061	101.7
178.0	9.9858	80.0
179.0	16.7417	67.4
179.125	18.5874	65.4
179.250	21.0570	63.4
179.375	24.4300	61.4
179.500	29.3185	58.6
179.625	37.0445	55.4
179.750	51.0667	50.9
179.875	83.7192	44.4
179.9062	99.3673	37.9
179.9375	120.4900	28.8
179.9688	141.6400	14.8
180.0	—	—

Table 3 Crossflow—boundary region solution

ϕ (DEG.)	$(g_\eta)_{MAX}$	w_{MAX}(FT/SEC.)
0.0	0.0	0.0
4.5	1.590	18.07
9.0	1.598	35.8
27.0	1.602	107.0
45.0	1.620	176.0
63.0	1.657	240.0
81.0	1.717	296.0
99.0	1.801	334.5
117.0	1.916	345.0
135.0	2.085	317.0
144.0	2.305	293.0
153.0	2.46	251.0
161.0	2.76	204.5
170.0	3.57	143.0
173.0	4.23	119.0
175.0	5.16	104.0
177.0	7.06	85.6
178.0	8.45	67.6
179.0	9.37	38.7
179.2	10.25	31.8
179.4	10.32	24.0
179.6	10.50	16.5
179.8	10.70	8.25
179.9	10.80	4.13
180.0		0.0

some ways similar to a corner geometry with the boundary condition $w=0$. The boundary-layer equations lead to an initial value problem in the azimuthal or φ direction and therefore cannot assure the satisfaction of the leeplane boundary condition. For very small incidence angles, boundary-layer theory is adequate in the vicinity of the leeplane as both marching and symmetry plane solutions satisfying the leeplane boundary condition exist. For larger incidence angles with increased mass accumulation at the leeplane, the $w=0$ boundary condition can no longer be satisfied in the marching procedure. The similarity symmetry plane calculations do not converge (Sec. III A) and the nonsimilar symmetry plane calculations lead to an unrealistic boundary-layer growth and predict a physically unacceptable streamwise separation (see Fig. 7). These results are indicative of boundary region formation or of a strong viscous-inviscid interaction and the loss of outer conical flow conditions. Although the latter may be important, it will be shown here that unique solutions for the leeplane can be obtained with a nonsimilar boundary region formulation and conical outer flow conditions. Agreement with experimental data is quite good. The boundary region equations[16] are of boundary value type in φ and therefore the leeplane boundary condition can be satisfied.

For larger incidence angles when crossflow reversal occurs and the separation line moves off the leeplane, symmetry plane solutions reappear (Sec. III C); it would appear that boundary region analysis is no longer important. As was shown in Sec. III C, the symmetry plane boundary-layer solutions are not in good agreement with experimental data;

solutions obtained with the boundary region formulation lead to a significant increase in accuracy. It therefore is concluded that for all but the smallest incidence angles boundary region analysis is necessary for laminar flows in order to satisfy the leeplane boundary condition. For large incidence the boundary region formulation is necessary as crossflow diffusion terms are important in the vicinity of the symmetry plane. The neglect of these terms does not invalidate the solution, but leads to a considerable loss of accuracy.

The windplane, although also cornerlike, is always an outflow plane with streamlines moving away from this symmetry plane. Therefore, the initial value nature of the boundary-layer equations is compatible with the windplane behavior and boundary regions never form at this symmetry plane.

For the experimental conditions of Tracy,[21] $M_\infty = 7.95$, $\alpha = 4°$, $K \approx -0.2444$, a detailed study of the leeplane behavior with both a nonsimilar boundary region[17] and a similar boundary-layer wind-to-leeplane marching procedure[11] was performed. It should be recalled once again that solutions of the uncoupled similarity equations do not exist for this K value (see Sec. III A) and the nonsimilar uncoupled leeplane equations lead to a fictitious streamwise separation, which does not occur with the boundary region solution (see Fig. 7). The results of this study, which confirm all previous postulates concerning the failure of boundary-layer theory for $-\bar{K} > K > -K^*$, now are presented. Figures 8 and 9 depict the profiles of the streamwise (f_η) velocities at several azimuthal locations around the cone. Nonsimilar boundary region and similar wind-to-leeplane boundary-layer solutions are compared. Significantly, for $\varphi \leq 175°$, the similar and nonsimilar solutions are in reasonable agreement in the inner boundary layer. Near the edge, the azimuthal diffusion terms are comparable to the decaying normal diffusion contributions and therefore somewhat larger variations are apparent. As $\varphi \to \pi$, the boundary region and boundary-layer profiles begin to differ significantly so that at $\varphi = 179°$ (Fig. 9) there is no correlation between the two solutions. Similar behavior is found for the crossflows. See Ref. 11 for additional results.

These differences are seen more dramatically on Tables 2 and 3 where the values of $(g_\eta)_{\max}$ and $(w)_{\max}$ are given for small increments near the leeplane. As the leeplane is approached, the boundary region solution for $w_{\max}$ predicts a rapid, but smooth, almost linear decay to zero. The large gradient from $\varphi = 178°$ to $\varphi = 180°$ establishes the existence of a boundary region. With crossflow diffusion neglected for the boundary-layer calculation the crossflow velocity exhibits much larger azimuthal gradients near the leeplane and the zero boundary condition cannot be satisfied, even with the small grid sizes considered here. The necessity of a boundary region formulation to resolve this leeplane singular behavior is apparent.

It is significant that even for $\varphi = 179°$, where Fig. 9 shows a dramatic difference in the boundary-layer and boundary region profiles, at the surface there is a small sublayer where the solutions are in moderate agreement and nearly similar. Therefore, both the boundary-layer ($\varphi < 180°$) and the boundary region ($\varphi \leq 180°$) solutions are acceptable for the surface heat transfer. Additional solutions are presented in Refs. 11 and 22. In Refs. 22 and 23 there is some discussion of turbulent boundary-layer behavior near the symmetry planes.

IV. Summary

Laminar flow in the symmetry planes of cones at angle of attack has been considered. The analysis and numerical solutions provide the following conclusions.

1) Windward plane solutions are obtained for all incidence angles $\alpha/\theta \leq 2$ with similarity boundary-layer theory. These uncoupled symmetry plane solutions are not unique, but for nonporous walls a unique branch can be inferred.

2) Multiple leeplane similarity solutions exist for very small incidence angles but for intermediate values of α/θ solutions fail to exist. Moreover, nonsimilar solutions are also unacceptable. For this range of incidence angle, a nonsimilar boundary region forms at the leeplane and cross-diffusion effects must be retained. Unique boundary region solutions are in good agreement with experimental data.

For large incidence angles similarity solutions of the uncoupled symmetry plane equations reappear, but are once again nonunique. Nonsimilar solutions are unique but are in poor agreement with experimental data. Unique boundary region solutions are once again in excellent agreement with the data.

For very large incidence $\alpha/\theta > 1$, nonunique "similarity" solutions of a sort still are obtained; however, they exhibit anomalous behavior near the boundary-layer edge where nonsimilar effects must be retained. This has been demonstrated with an asymptotic analysis of the nonsimilar boundary-layer equations as well as nonsimilar numerical solutions. Once again agreement with experiment is poor, but is improved considerably when boundary region effects are retained. Therefore the boundary region at the leeplane is important for all but the smallest incidence angles.

Acknowledgment

This research was supported by the Air Force Office of Scientific Research under Grant AFOSR 74-2635, Project 9781-01.

References

[1]Moore, F. K., "Laminar Boundary Layer on Cones in Supersonic Flow at Large Angle of Attack," NACA TN 2844, Nov. 1952.

[2]Cheng, H. K., "The Shock Layer Concept and Three-Dimensional Hypersonic Boundary Layers," Rep. AF-1285-A-3, 1961, Cornell Aeronautical Laboratory, Ithaca, N. Y.

[3]Roux, B., "Supersonic Laminar Boundary Layer Near the Plane of Symmetry of a Cone at Incidence," *Journal of Fluid Mechanics*, Vol. 51, Pt. 1, 1972, pp. 1-14.

[4]Murdock, J. W., "The Solution of Sharp Cone Boundary Layer Equations in the Plane-of-Symmetry," TR-0172 (S2816-60)-1, 1971, Aerospace Corp., El Segundo, Calif.

[5]Wu, P. and Libby, P. A. "Laminar Boundary Layer on a Cone Near a Plane of Symmetry," *AIAA Journal*, Vol. 11, March 1973, pp. 326-333.

[6]Reshotko, E., "Laminar Boundary Layer with Heat Transfer on a Cone at Angle of Attack in a Supersonic Stream," NACA TN 4152, Dec. 1957.

[7]Eaton, R. R and Larson, D. E., "Laminar and Turbulent Viscous Shock Layer Flow in the Symmetry Planes of Bodies at Angle of Attack," AIAA Paper 74-599, Palo Alto, Calif., 1974.

[8]Cooke, J. C., "Supersonic Laminar Boundary Layer on Cones," Rep. No. 66347, 1965, Royal Aircraft Establishment, Farnborough, England.

[9]Boericke, R. R., "The Laminar Boundary Layer on a Cone at Incidence in Supersonic Flow," *AIAA Journal*, Vol. 9, March 1971, pp. 462-468.

[10]Roux, B., "Etude Theorique de l'Effet de l'Incidence sur la Couche Limite Laminaire Autour d'un Cone Circulair," *Journal de Mecanique*, Vol. 10, 1971, pp. 467-502.

[11]Tarulli, F., "The Boundary Layer on a Cone at Angle of Attack," M. S. Thesis, 1974, Polytechnic Institue of New York, Brooklyn, N. Y.

[12]Popinski, Z. and Davis, T., "Three-Dimensional Compressible Laminar Boundary Layer on Sharp and Blunt Cones," NASA CR-112316, 1973.

[13]Mayne, A. A., "Analysis of Laminar Boundary Layers on Right Circular Cones at Angle of Attack Including Streamline Swallowing Effects," AECD-TR-72-134, 1972, Arnold Engineering Development Center, Wright-Patterson, AFB, Ohio.

[14]Adams, J., "Analysis of the Three-Dimensional Compressible Turbulent Boundary Layer on a Sharp Cone at Incidence in Supersonic and Hypersonic Flow," AECD-TR-72-66, 1972, Arnold Engineering Development Center, Wright-Patterson AFB, Ohio.

[15]Harris, J. and Morris, D., "Solution of the Three-Dimensional Compressible Laminar and Turbulent Boundary-Layer Equations," *Fourth International Conference on Numerical Methods in Fluid Dynamics*, Boulder, Colo., 1974.

[16]Lin, T. C. and Rubin, S. G., "Viscous flow Over a Cone at Incidence I-Hypersonic Tip Region," *Computer and Fluids*, Vol. 1 1972, pp. 37-57.
[17]Lin, T. C. and Rubin, S. G., "Viscous Flow Over a Cone at Incidence, II-Supersonic Boundary Layer," *Journal of Fluid Mechanics*, Vol. 59, pp. 593-620.
[18]Lubard, S. and Helliwell, W., "Calculation of the Flow on a Cone at High Angle of Attack," *AIAA Journal*, Vol. 12, July 1974, pp. 965-974.
[19]Rubin, S. G. and Grossman, B., "Viscous Flow Along a Corner," *Quarterly of Applied Mathematics*, Vol. 24, 1971, pp. 169-186.
[20]Rubin, S. G. and Mummolo, F. J., "Boundary-Layer-Induced Potential Flow on an Elliptic Cylinder," *Journal of Fluid Mechanics*, Vol. 66, Pt. 1, 1974, pp. 145-157.
[21]Tracy, R. "Hypersonic Flow Over a Yawed Cone," CALCIT Memo. No. 69, 1963, California Institute of Technology, Pasadena, Calif.
[22]Rubin, S. G., Lin, T. C., and Tarulli, F., "The Viscous Layer in the Symmetry Plane of Sharp Cone at Incidence," POLY AE/AM Rept. No. 75-8, 1975, Polytechnic Institute of New York, Brooklyn, N.Y.
[23]Lin, T. C., and Rubin, S. G., "A Two-Layer Model for a Coupled Three-Dimensional Viscous and Inviscid Flow Calculation," AIAA Paper 75-853, June 16-18, 1975, Hartford, Conn.